15A.1 LOCAL ROUGHNESS EFFECTS ON TORNADO DYNAMICS

D. C. Lewellen*
West Virginia University, Morgantown, WV.

1 INTRODUCTION

To estimate what damage a tornado measured over open plains might have produced had that tornado passed instead over a large structure or group of structures, it is common to simply superpose the measured wind fields over the new environment (e.g., Wurman et al. (2007)). One should, however, also consider how the presence of the structures, or more generally any localized surface roughness elements, might themselves alter the tornado wind fields. The known sensitivity of the tornado cornerflow to properties of the near- surface inflow suggest that such effects could at times be significant. It has long been appreciated that an increase in general surface roughness will alter tornado cornerflow structure toward that for a vortex characterized by a lower swirl ratio (e.g., Leslie (1977); Lewellen et al. (2000)), but the effects of very local changes in roughness have not, to our knowledge, been previously considered. Deducing such effects by observing the behavior of actual tornadoes transitioning between different environments (or the changes in the damage tracks they leave behind) is problematic because of the natural unsteadiness of tornado behavior due to other effects such as changes in conditions aloft. Here we use large eddy simulations (LES) and simple theoretical models to help isolate possible effects of local roughness elements.

2 APPROXIMATE TORNADO SURFACE LAYER DYNAMICS

The outer conditions of the simulations (away from the surface and vortex core) are taken with a constant angular momentum (Γ_∞) and constant horizontal convergence (a_c). This provides an exact inviscid solution of the incompressible Navier-Stokes equation with perturbation pressure p and velocity components u, v, w (radial, azimuthal, vertical) of:

$$p = -\frac{1}{2}(\frac{\Gamma_\infty^2}{r^2} + a_c^2 r^2) - 2a_c^2 z^2 \quad (1)$$

$$u = -a_c r \quad (2)$$
$$v = \Gamma_\infty / r \quad (3)$$
$$w = 2a_c z \quad . \quad (4)$$

For convenience we have chosen mass units such that the density $\rho = 1$ drops out of the equations. For a simplified model of the surface layer consider first a smooth surface with a layer of reduced angular momentum, Γ_1, between it and the Γ_∞ region aloft (arising perhaps from surface friction at larger radii). In the inviscid approximation the Bernoulli constant (or total head, H_1), Γ_1 and radial flux (Φ) in this layer are all conserved as this fluid flows inward (given the assumed smooth surface). Further, for modest layer thickness and away from the core, the boundary-layer approximation is valid so that $dp/dz = 0$ in the layer, so p is known from the solution aloft. One can then simply solve for the velocity components within the layer and the layer depth h_1 as a function of radius:

$$u_1 = [2H_1 + \frac{\Gamma_\infty^2 - \Gamma_1^2}{r^2} + a_c^2 r^2]^{1/2} \quad (5)$$
$$v_1 = \Gamma_1 / r \quad (6)$$
$$h_1 = \Phi/(2\pi r u_1) \quad . \quad (7)$$

Generally the cases and regions of most interest are when r is small enough that the swirl terms dominate the convergence terms in p and $|p|$ dominates $|H_1|$ so to good approximation we have,

$$u_1 \approx \sqrt{\Gamma_\infty^2 - \Gamma_1^2}/r \quad (8)$$
$$h_1 \approx \Phi/(2\pi\sqrt{\Gamma_\infty^2 - \Gamma_1^2}) \quad . \quad (9)$$

Thus the magnitudes of u_1 and v_1 both increase as $1/r$ with decreasing r, but the angle of the boundary layer flow and its depth h_1 do not change (features seen to good approximation over the relevant regions in the simulations even with more realistic conditions). This solution holds until the vortex core radius is approached. The structure in this cornerflow region is largely governed by the cornerflow swirl ratio (Lewellen et al., 2000),

$$S_c = r_c \Gamma_\infty^2 / \Upsilon \quad , \quad (10)$$

where r_c is the vortex core radius above the cornerflow region and Υ is the depleted angular momentum flux

*Corresponding author address: D. C. Lewellen, MAE Dept. PO Box 6106, WVU, Morgantown, WV, 26506-6106; e-mail: dclewellen@mail.wvu.edu.

flowing through the region. In the simple model above $\Upsilon = (\Gamma_\infty - \Gamma_1)\Phi$ leading to a simple relation between S_c, r_c and h_1:

$$S_c \approx \frac{r_c}{2\pi h_1} \quad . \tag{11}$$

This agrees with the qualitative structure one expects in the cornerflow: a shallow inflow layer relative to the core radius aloft for "high-swirl" conditions; a relatively deep one for "low-swirl".

For less idealized surface layers (e.g., a smooth Γ profile rather than a discontinuous step in z) Υ is more easily defined unambiguously than Φ and h_1 so it is convenient, for purposes of general scaling arguments, to define characteristic scales of the latter in terms of the former by matching results for the simplest $\Gamma_1 = 0$ version of the model above,

$$\Upsilon(r) \equiv \int dz 2\pi r u(r,z)(\Gamma_\infty - \Gamma(r,z)) \tag{12}$$

$$\Phi \sim \Upsilon/\Gamma_\infty \tag{13}$$

$$h_1 \sim \Upsilon/(2\pi\Gamma_\infty^2) \quad . \tag{14}$$

Now consider the effects of individual surface roughness elements in this simple model. We assume these to be arrayed sparsely on the surface (so that their contributions may be considered approximately independent of each other) but uniformly enough that approximate axisymmetry of the inflow will persist. We assume the vortex translation speed to be negligible, again for the sake of approximate axisymmetry. Each element acts as a sink of angular momentum and hence a source of Υ. The drag force exerted by each element on the flow is given by,

$$\vec{F_d} = -\frac{1}{2} C_d A_b |\vec{u_b}| \vec{u_b} \quad , \tag{15}$$

where $\vec{u_b}$ is the unperturbed wind velocity at the elements position, A_b is the projected cross-sectional area of the element and C_d is the drag coefficient, which for a bluff body is nearly independent of Reynold's number and $C_d \approx 1$. Each element acts as a sink for angular momentum, with the change in radial flux of angular momentum (i.e., the net increase in Υ due to the element) equal to the torque exerted by the element integrated over its extent. Then for a block element of height z_b located a distance r_b from the tornado axis (and again assuming the swirl dominated regime where $|p|$ dominates $|H_1|$),

$$\delta\Upsilon = \int (\vec{r} \times \vec{F_d}) \cdot \hat{z} \approx \frac{C_d A_b \Gamma_\infty}{2 r_b} \frac{1}{z_b} \int_0^{z_b} dz \Gamma(r,z) \quad . \tag{16}$$

In the limit of tall sparse elements stretching well into the Γ_∞ layer this becomes of order (dropping C_d as well),

$$\delta\Upsilon \approx \frac{A_b \Gamma_\infty^2}{2 r_b} \quad . \tag{17}$$

The addition of a tornado translation speed alters the relative velocity between the element and the tornado center, either increasing or decreasing the change in Υ depending on whether the element lies to the right or left of the tornado path (assuming counter-clockwise rotation). In the limit where the swirl velocity dominates the translation velocity (17) is modified to,*

$$\delta\Upsilon \approx \frac{A_b (\Gamma_\infty \pm u_t y_b)^2}{2 r_b} \quad , \tag{18}$$

for translation velocity u_t and transverse distance y_b between the element and the tornado path (using the plus sign if it lies to the right and minus sign if it lies to the left).

From this rough approximation and the definition (10) we can estimate that for a single roughness element to have a significant effect on S_c we must have $\delta\Upsilon$ non-negligible relative to $r_c \Gamma_\infty^2 / S_c$. Since changes in S_c have their greatest effects on near-surface tornado structure and intensity when S_c has a value around the low-swirl peak ($S_c^* \approx$1.2-1.5)(Lewellen et al., 2000) rather than for $S_c \gg 1$, we can express this alternatively that a single roughness element will significantly impact the near-surface tornado structure and intensity if,

$$A_b / r_b \sim r_c \quad . \tag{19}$$

Note that the increase of a roughness element's effects with decreasing r_b will not generally continue for $r_b \ll r_c$ because the winds encountered do not continue to grow (and in a large high-swirl tornado may drop off significantly).

Several observations can be drawn from this simple analysis. There are three basic length scales of the roughness elements (object height, width, and distance from the tornado) and three basic length scales of the tornado (core size, inflow layer depth, and radial extent over which swirl dominates the inflow aloft, $r_s \sim \sqrt{\Gamma_\infty / a_c}$) that play a role. Because low-level wind speeds scale roughly as $1/r$, the effects of individual roughness elements on the tornado increase greatly as their distance from the tornado (relative to the tornado core size) decreases; however, for a quasi-uniform coverage of roughness elements over the surface the effects of the far-field elements in aggregate will dominate because of the increase in number involved (area scaling as r^2). The integrated far-field

*Note that unlike in the axisymmetric case, in the presence of a translation much of the near-surface flow at large radius (where the translation velocity might easily exceed the swirl velocity) will not be channeled into the vortex core and thus not contribute to Υ.

effects may either weaken or strengthen the tornado near the surface, depending on S_c. Far field elements will have an impact only as long as they are within the convergence region feeding the vortex core (out to $\sim r_s$) and the effects may largely saturate if the layer depth grows deep enough ($h_1 \sim z_b$).

3 SIMULATION APPROACH

For the simulations considered here, a limited volume (2×2×3 km^3) was employed, with different choices of steady converging swirling inflows (rotating cyclonically) applied at the boundaries to produce different types of turbulent vortices within. Simple block "buildings", either singly or in arrays, were included using the "Immersed Boundary Method" (IMB). The implementation of the IMB used was essentially that which we employed earlier for incorporating smooth topography (Lewellen, 2010) with, however, one important difference. Since the IMB involves a continuation of the flow solution within the solid with forcing terms included to implement the flow boundary conditions implicitly at the immersed surface, it works best for smooth surfaces. At high Reynolds numbers (where we cannot assume all velocities become small around the boundary) it becomes problematic for boundaries with discontinuous slopes unless the boundaries coincide with grid boundaries for the normal velocity components. Accordingly simulations with translating tornadoes and blocks were performed in a reference frame fixed with the blocks, with time varying conditions set on the domain boundaries consistent with the tornado translation. High resolution and numerical efficiency were retained by using an extended central fine grid region and keeping the tornado core within that region by performing the simulations in two or three segments over time, imposing finite domain shifts between the grids used. The methods were checked against control runs using the same procedures without blocks as well as against ones with blocks and stationary tornadoes.

In addition to the block elements a uniform background surface roughness could be included defined by a surface roughness length z_0, assuming a turbulent log-layer boundary layer below the first vertical grid point of the simulation. The roughness of the block faces themselves were, for simplicity, considered to be negligible. Other details of the model and simulation procedures may be found in Lewellen et al. (2008) and references therein.

One challenge in trying to study surface roughness effects with limited domain simulations is that for some conditions surface changes will strongly affect the core flow and result in a physical feedback involving the core even far above the corner flow. To allow this feedback to occur in physically realistic fashion independent of the details of the boundary conditions chosen at the domain top we simulated, in many cases, nested circulations on inner and outer scales as in fig 1. This may be considered as an idealized version of a tornado circulation within a mesocyclone circulation. These were produced as described in Lewellen and Lewellen (2007a) (see e.g., fig. 3 there). The inner vortex is driven by the convergence into the larger-scale vortex corner flow. As a result the simulated tornado vortex core "terminates" aloft within the domain in a physically realistic way.

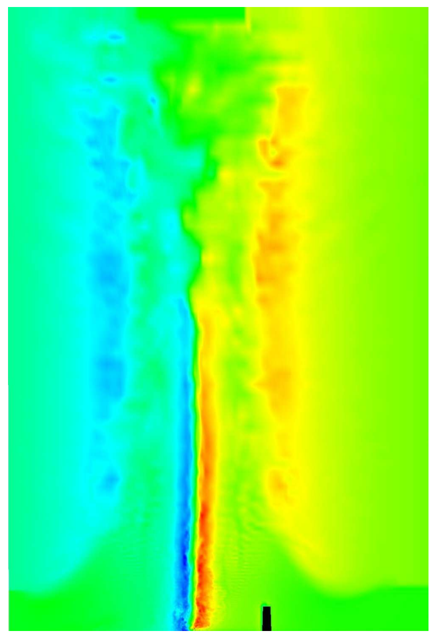

Figure 1: Swirl velocity on a central slice through the full simulation domain showing nested inner and outer circulations. A 120 m tall block element is included.

Of order ∼150 simulations were performed varying tornado swirl ratio, size, and translation speed and block dimensions, number and placement. Finest grid resolutions were 4 m in the horizontal and 1 m in the vertical.

Important caveats to the study include the absence of storm-scale effects and that the blocks were treated as static and impermeable with no debris effects considered. Clearly for some conditions wind-induced damage could change the aerodynamics of the surface structures significantly and hence change both the effects on the tornado and the pressure forces the structures are subjected to.

4 SAMPLE SIMULATION RESULTS

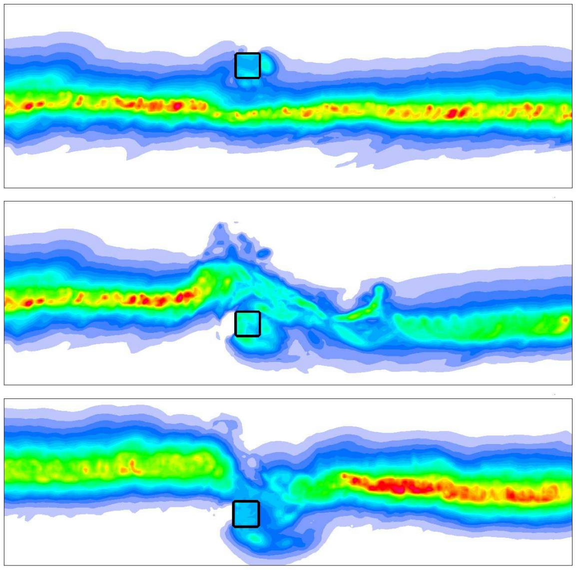

Figure 2: Surface tracks of peak pressure drop encountered at 3 m height for sample simulated medium swirl tornadoes moving left to right. Block dimensions are 40×40×120 m. Ratio of translation velocity to core swirl velocity aloft is $u_t/v_c \approx .4$ (top and middle); $u_t/v_c \approx .15$ (bottom).

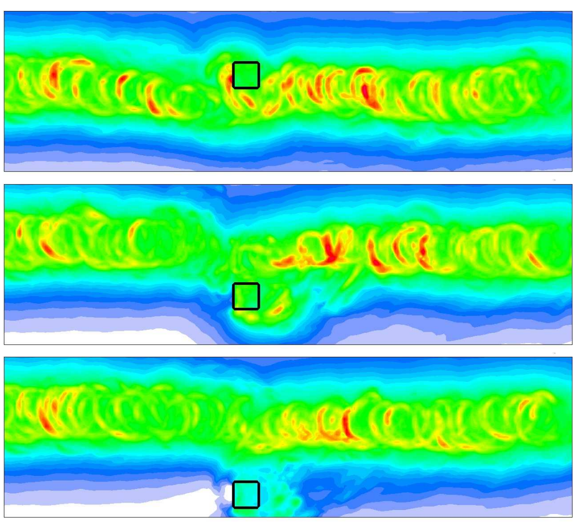

Figure 3: Surface tracks of peak pressure drop encountered at 3 m height for sample simulated high swirl tornadoes. Block dimensions are 40×40×120 m; $u_t/v_c \approx .15$.

Figures 2-3 show sample results for cases with only a single block roughness element (e.g., a large building) as viewed from "tracks" of the peak near-surface pressure drops encountered over time as the simulated tornado translates over the surface. Figure 4 gives some further examples with simulated vortices interacting with an array of block elements. Several of the features predicted by the simple surface analysis given above are readily apparent: the effects of the block are slight if r_b is much greater than r_c but can be very large when (19) is satisfied; the effects are significantly larger for blocks lying to the left of the tornado path than those to the right when the tornado is rapidly translating; smaller blocks give smaller effects; and the effects of a block on the main vortex are less for larger r_c.

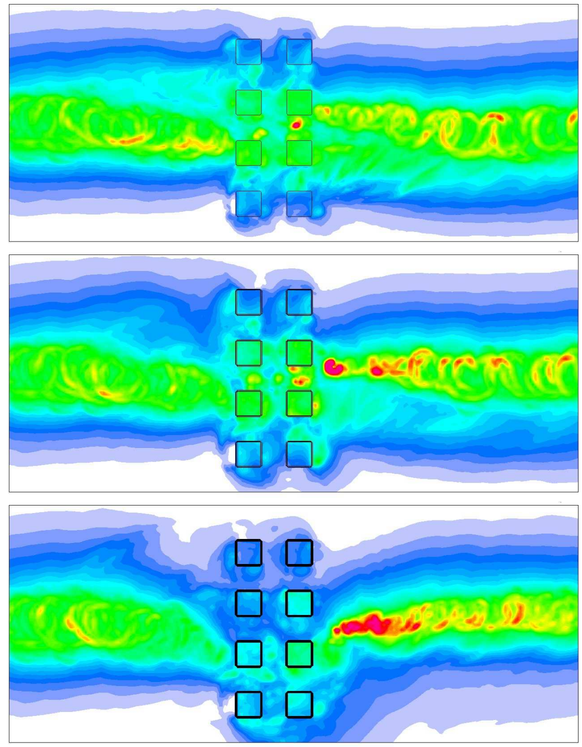

Figure 4: Surface tracks as in fig. 3 but over arrays of 40×40 m blocks of heights 20 m (top), 40 m (middle), 120 m (bottom).

The presence of a block (or blocks) can lead to regions of intensification or deintensification near the surface (or both). The axisymmetric analysis would predict that an increases in Υ from a block would effectively decrease the corner flow swirl ratio, leading to a net increase in intensity near the surface (but contracted footprint) unless (or until) S_c is pushed well below S_c^*, blowing out the core at the surface and dropping the near-surface intensification. Qualitatively these expectations seem properly reflected in the simulation results but there are other factors (not consid-

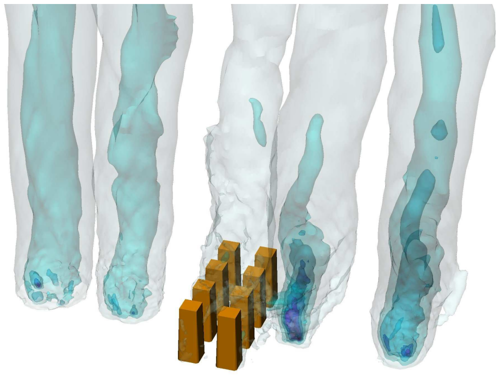

Figure 5: Evolution of the bottom frame case of fig. 4 as visualized with nested perturbation pressure isosurfaces sampled at equally spaced time intervals.

ered in the simple theoretical model above) that lead to a much richer array of effects. Among the most important are transient effects. The response from approaching and then receding from a block (first increasing and then decreasing Υ into the corner flow) does not lead to a symmetric response because the transient increase in Υ affects the core flow throughout the subsequent evolution, sometimes leading to a transient overshoot in near-surface intensification downstream of the blocks (e.g. fig. 2 bottom frame, fig. 4 bottom frame, fig. 5) – an example of "corner flow collapse" intensification (Lewellen and Lewellen, 2007b). Other effects include: deviations from axisymmetry due to the presence of the block causing deflections in the tornado path at the surface; angular momentum losses from tall near-by blocks feeding directly into the core aloft without passing through the surface layer (weakening the cornerflow below); and disruption or enhancement of secondary vortices. The latter effects are particularly important for high-swirl tornadoes with large r_c: A_b/r_b may be significant relative to the size of a secondary vortex even when it is dwarfed by the scale of the primary vortex. This can lead to significant weakening of secondary vortices. Occasionally, however it can lead to a stronger secondary vortex downstream, starting from a vortex shed in the block's wake.

5 PRESSURE FORCES ON BUILDING FACES

While the emphasis in this study has been on the effects of "buildings" on the tornado flow, the pressure forces exerted by the tornado on a building are obviously of critical interest. For the simulation set, time histories of the pressure distributions on the block surfaces were collected. Figures 6 and 7 show sample results from one case. Net forces on the blocks tend to

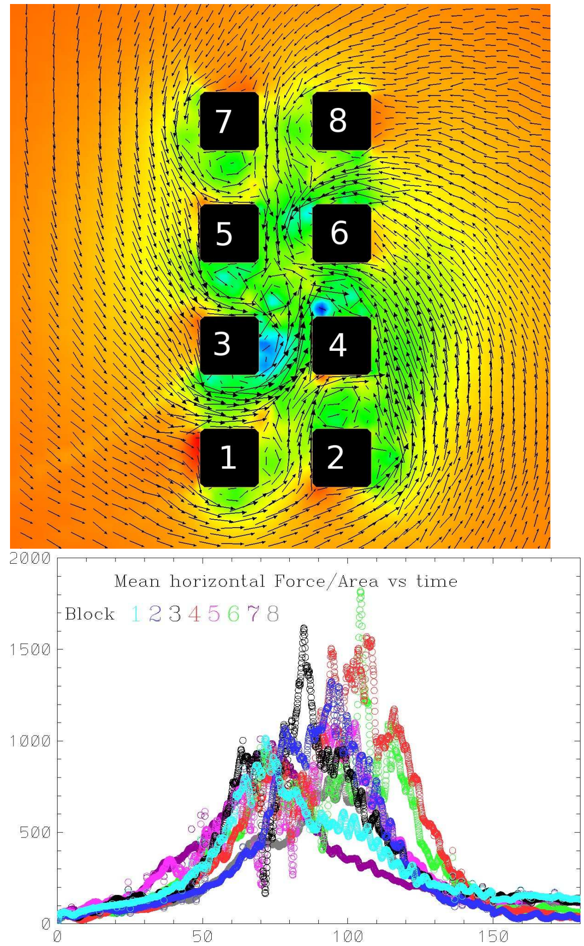

Figure 6: Bottom frame: time history of integrated net horizontal force per area on different blocks (block 1 light blue, 2 dark blue, 3 black, 4 red, 5 light purple, 6 green, 7 dark purple, 8 grey). Blocks as labeled in the top frame showing also horizontal wind vectors and near-surface pressure at time 84 s when the vortex is centered over the block array. The case is that of the middle frame of fig. 4.

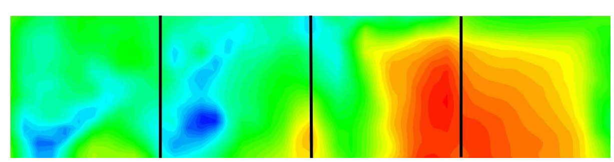

Figure 7: Perturbation pressure distribution on the South, East, North and West faces of block-3 at 84 s shown in fig. 6

fluctuate significantly in time, both in magnitude and direction. The spatial fluctuations in the wind-induced pressure distributions on individual block faces tend to be significant as well (the variances being typically of the same order as the mean), so local forces can be expected to significantly exceed mean forces much of the time. For a given position relative to the tornado, total forces on single blocks scale roughly with the block area unless the blocks are large enough to significantly affect the tornado strength, whereupon the force per area on the block tends to drop. It is an interesting consequence of the flow geometry that in some circumstances a block can effectively shield itself to some extent from the strongest winds. As expected the mean force on tall (relative to h_1) blocks is dominantly from the swirl component but veers toward the radial for shorter blocks. From the initial inspection of the results few general rules about the pressure forcing (such as which positions in block arrays might generally encounter greater or lesser forcing) are apparent across the simulation set. The utility of the results for assessing the failure modes of actual structures is substantially limited by treating the blocks as impermeable: the actual forces on building segments would depend as well on the pressure response within the buildings (which may be expected to vary significantly depending on building volume and tornado translation speed) and on aerodynamic changes due to structural damage.

6 CONCLUSIONS

A large simulation set together with simpler analytic estimates suggest that individual roughness elements can lead to significant local weakening and/or strengthening of a tornado if large enough and close enough ($A_b/r_b \sim r_c$). The effects are largest on low or medium swirl tornadoes and on secondary vortices within high swirl tornadoes. For tornadoes with significant translation velocities the effects are greatest for elements on the right side of the tornado path where the swirl and translation velocities are aligned. While the simulations suggest that large buildings might sometimes shield themselves and other local structures from the strongest tornado winds, we stress that they do not support any general conclusions about city environments providing protection from tornadoes: a large enough high-swirl tornado would not be appreciably weakened and the presence of large buildings could in some circumstances lead to more damaging winds in some locations from modest sized tornadoes.

7 ACKNOWLEDGMENTS

This material is based upon work supported by the National Science Foundation, under Grant 1013154.

References

Leslie, F. W., 1977: Surface roughness effects on suction vortex formation: a laboratory simulation. *J. Atmos. Sci.*, **34**, 1022–1027.

Lewellen, D. C., 2010: Effects of topography on tornado dynamics: A simulation study. *Preprints, 26th Conference on Severe Local Storms*, AMS, Nashville, TN, paper 4B.1.

Lewellen, D. C., B. Gong, and W. S. Lewellen, 2008: Effects of fine-scale debris on near-surface tornado dynamics. *J. Atmos. Sci.*, **65**, 3247–3262.

Lewellen, D. C., and W. S. Lewellen, 2007a: Near-surface intensification of tornado vortices. *J. Atmos. Sci.*, **64**, 2176–2194.

Lewellen, D. C., and W. S. Lewellen, 2007b: Near-surface vortex intensification through corner flow collapse. *J. Atmos. Sci.*, **64**, 2195–2209.

Lewellen, D. C., W. S. Lewellen, and J. Xia, 2000: The influence of a local swirl ratio on tornado intensification near the surface. *J. Atmos. Sci.*, **57**, 527–544.

Wurman, J., C. Alexander, P. Robinson, and Y. Richardson, 2007: Low-level winds in tornadoes and potential catastrophic tornado impacts in urban areas. *Bull. Amer. Meteor. Soc.*, **88**, 31–46.